DALTON
FULL PAPER

Intramolecular hydrogen bonding between 2-cyanoguanidine and 3-chloro-6-(pyrazol-1-yl)pyridazines in copper(II) complexes

Alexander J. Blake, Peter Hubberstey,*† Wan-Sheung Li, Claire E. Russell, Beverley J. Smith and Louise D. Wraith

Chemistry Department, Nottingham University, Nottingham, UK NG7 2RD

Treatment of copper(II) salts with 3-chloro-6-(pyrazol-1-yl)pyridazine (cppd)–2-cyanoguanidine (cnge) mixtures yielded $[Cu(cppd)_2(H_2O)_2][NO_3]_2$, $[Cu(cppd)(cnge)_2(H_2O)(FBF_3)][BF_4]$, $Cu(cppd)_2Cl_2{\cdot}2H_2O$ and $Cu(cppd)_2Br_2{\cdot}2H_2O$. The corresponding 3-chloro-6-(3,5-dimethylpyrazol-1-yl)pyridazine (cmppd) systems gave $Cu(cmppd)(cnge)_2(NO_3)_2{\cdot}6H_2O$, $[Cu(cmppd)_2(cnge)][BF_4]_2$, $[Cu(cmppd)(cnge)Cl_2]{\cdot}H_2O$ and $Cu(cmppd)(cnge)Br_2{\cdot}H_2O$. Four of the complexes have been structurally characterised. Whereas the copper atoms in $[Cu(cppd)_2(H_2O)_2][NO_3]_2$ and $[Cu(cppd)(cnge)_2(H_2O)(FBF_3)][BF_4]$ have tetragonally elongated distorted octahedral geometry, those in $[Cu(cmppd)_2(cnge)][BF_4]_2$ and $[Cu(cmppd)(cnge)Cl_2]{\cdot}H_2O$ adopt trigonal-bipyramidal geometries. The centrosymmetric $[Cu(cppd)_2(H_2O)_2]^{2+}$ cation comprises two equatorial bidentate chelating cppd ligands and two axial water molecules while $[Cu(cppd)(cnge)_2(H_2O)(FBF_3)]^+$ comprises one cppd and two monodentate cnge molecules as equatorial ligands and one water molecule and one BF_4^- anion as axial ligands. In the $[Cu(cmppd)(cnge)Cl_2]$ molecule the chlorine atoms occupy equatorial sites, the cnge an axial position and the cmppd ligand straddles equatorial and axial sites, while in the $[Cu(cmppd)_2(cnge)]^{2+}$ cation the cnge ligand is located equatorially and the two cmppd ligands straddle equatorial and axial sites. Preliminary structural data for $Cu(cppd)_2Br_2{\cdot}2H_2O$ are consistent with a centrosymmetric tetragonally elongated octahedral copper atom similar to that in $[Cu(cppd)_2(H_2O)_2][NO_3]_2$. Comparable IR and UV/VIS data were obtained for $Cu(cmppd)(cnge)_2(NO_3)_2{\cdot}6H_2O$ and $[Cu(cppd)(cnge)_2(H_2O)(FBF_3)][BF_4]$ and for $Cu(cmppd)(cnge)Br_2{\cdot}H_2O$ and $[Cu(cmppd)(cnge)Cl_2]{\cdot}H_2O$, suggesting similar molecular structures. Intramolecular N–H···N hydrogen bonds occur between cnge amino groups and pyridazine non-ligating nitrogens in the mixed-ligand complexes $[Cu(cppd)(cnge)_2(H_2O)(FBF_3)][BF_4]$ and $[Cu(cmppd)(cnge)Cl_2]{\cdot}H_2O$ but not $[Cu(cmppd)_2(cnge)][BF_4]_2$. That in $[Cu(cppd)(cnge)_2(H_2O)(FBF_3)][BF_4]$ differentiates between the two cnge ligands, their different roles being confirmed by the presence of two diagnostic $\nu_{asym}(NCN)$ doublets in its IR spectrum.

Recognition of the role of hydrogen bonding in the crystal engineering of supramolecular structures[1–5] has resulted in a rapid expansion of interest in the topic. In a recent paper[2] we discussed the hydrogen-bonding flexibility of 2-cyanoguanidine (cnge) in a series of copper(II)–2,2′-bipyridine (2,2′-bipy)–cnge complexes, $Cu(2,2'\text{-bipy})(cnge)_2(NO_3)_2$ **1**, $[Cu(2,2'\text{-bipy})(cnge)_2(FBF_3)_2]$ **2**, $[Cu(2,2'\text{-bipy})_2(cnge)][BF_4]_2{\cdot}H_2O$ **3**, $[Cu(2,2'\text{-bipy})(cnge)Cl_2]{\cdot}H_2O$ **4** and $Cu(2,2'\text{-bipy})(cnge)Br_2{\cdot}H_2O$ **5**. Structural studies of **2**, **3** and **4** revealed intramolecular N–H···X interactions between co-ordinated cnge and co-ordinated anions in **2** and **4** but not **3** and diverse intermolecular interactions in all three complexes. The latter include (i) double N–H donor systems in which both amino groups of a cnge molecule provide contacts to separate acceptor atoms of an anion, typically BF_4^-, and (ii) paired donor–acceptor contacts between two (often centrosymmetric) cnge molecules in which each provides a donor and acceptor function.[2]

To probe further the role of hydrogen bonding in supporting the co-ordination of weakly co-ordinating anions (*e.g.* BF_4^-) in the weakly binding sites of copper(II) complexes we have considered the effect of incorporation of a hydrogen-bonding acceptor site in the bidentate chelating ligand. Thus, we now describe the synthesis and structural chemistry of the corresponding copper(II)–cnge–3-chloro-6-(pyrazol-1-yl)pyridazine complexes within which intramolecular N–H···N hydrogen bonds can form between the cnge amino moieties and not only the co-ordinated anions [Scheme 1(a)] but also the pyridazine non-ligating nitrogen [Scheme 1(b)]. We have synthesized and characterised a series of copper(II)–cnge–3-chloro-6-(pyrazol-1-yl)pyridazine (cppd) or 3-chloro-6-(3,5-dimethylpyrazol-1-yl)pyridazine (cmppd) complexes of differing stoichiometry (1 : 1 : 2, 1 : 1 : 1, 1 : 2 : 1) and with diverse anions (NO_3^-, BF_4^-, Cl^- or Br^-), namely $[Cu(cppd)_2(H_2O)_2][NO_3]_2$ **6**, $[Cu(cppd)(cnge)_2(H_2O)(FBF_3)][BF_4]$ **7**, $Cu(cppd)_2Cl_2{\cdot}2H_2O$ **8**, $Cu(cppd)_2Br_2{\cdot}2H_2O$ **9**, $Cu(cmppd)(cnge)_2(NO_3)_2{\cdot}6H_2O$ **10**, $[Cu(cmppd)_2(cnge)][BF_4]_2$ **11**, $[Cu(cmppd)(cnge)Cl_2]{\cdot}H_2O$ **12** and $Cu(cmppd)(cnge)Br_2{\cdot}H_2O$ **13**. Structural data have been obtained for **6**, **7**, **9**, **11** and **12**.

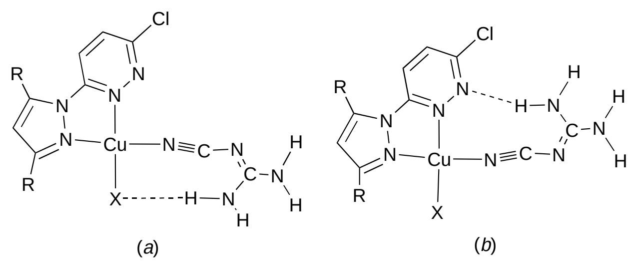

Scheme 1 Possible intramolecular hydrogen-bonding interactions in copper(II) complexes containing both 2-cyanoguanidine and pyrazole-substituted pyridazines. R = H, 3-chloro-6-(pyrazol-1-yl)pyridazine (cppd); R = Me, 3-chloro-6-(3,5-dimethylpyrazol-1-yl)pyridazine (cmppd); X = anion

Results and Discussion

The complexes were crystallised from the mixtures obtained by combining aqueous solutions of the appropriate copper(II) salt [$Cu(NO_3)_2{\cdot}3H_2O$, $Cu(BF_4)_2{\cdot}xH_2O$, $CuCl_2{\cdot}2H_2O$ or $CuBr_2$] and cnge with an acetonitrile solution of cppd or cmppd. The reaction chemistry is summarised together with that of the corresponding 2,2′-bipy system[2] in Scheme 2. Although there are

† E-Mail: peter.hubberstey@nottingham.ac.uk

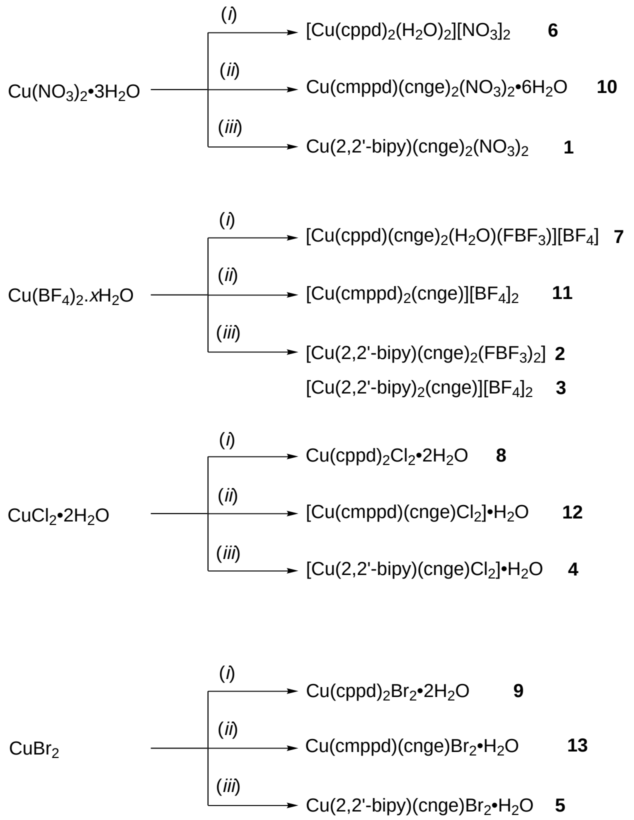

Scheme 2 Products of the reactions of copper(II) salts with diimine–2-cyanoguanidine mixtures [diimine = 2,2′-bipyridine or a 3-chloro-6-(pyrazol-1-yl)pyridazine]. (*i*) cppd, 2 cnge; (*ii*) cmppd, 2 cnge; (*iii*) 2,2′-bipy, 2 cnge

some recognisable trends, many anomalies occur. For cppd a mixed-ligand product (**7**) was only formed in the tetrafluoroborate system. The nitrate (**6**), chloride (**8**) and bromide (**9**) systems yield bis(cppd) complexes of identical stoichiometry, $Cu(cppd)_2X_2{\cdot}2H_2O$ (X = NO_3, Cl or Br). For cmppd all four salts yielded mixed-ligand products, but of differing cmppd : cnge stoichiometry; 1 : 2, 1 : 1, 1 : 1 and 2 : 1 complexes were formed by the nitrate (**10**), chloride (**12**), bromide (**13**) and tetrafluoroborate (**11**), respectively. All eight products were initially characterised by elemental analysis (C, H, N), magnetochemistry and IR and UV/VIS spectroscopy. X-Ray diffraction data were subsequently measured for **6**, **7**, **9**, **11** and **12**, resulting in unambiguous identification. Owing to the difficulty of ensuring complete combustion of copper complexes with high nitrogen content, the identities of **8**, **10** and **13** are less certain, but only in their water content.

Whereas complex **6** comprises $[Cu(cppd)_2(H_2O)_2]^{2+}$ cations and NO_3^- anions and **7** and **11** contain BF_4^- anions and, respectively, $[Cu(cppd)(cnge)_2(H_2O)(FBF_3)]^+$ and $[Cu(cmppd)_2(cnge)]^{2+}$ cations, **12** is based on the neutral complex, $[Cu(cmppd)(cnge)Cl_2]$. Complex **12** also contains an unco-ordinated water molecule. The molecular structures of the copper(II) complexes are shown in Figs. 1–5. Selected interatomic distances and angles are collected in Table 1; hydrogen-bonding interactions are summarised in Table 2. Two different copper(II) co-ordination geometries are adopted; whereas $[Cu(cppd)_2(H_2O)_2]^{2+}$ and $[Cu(cppd)(cnge)_2(H_2O)(FBF_3)]^+$ are tetragonally elongated octahedral, $[Cu(cmppd)(cnge)Cl_2]$ and $[Cu(cmppd)_2(cnge)]^{2+}$ are trigonal bipyramidal.

Crystal and molecular structure of complex 6

The co-ordination geometry of the copper atom in complex **6** (Fig. 1), which is located on an inversion centre, is typical of Jahn–Teller distorted octahedral (d^9) systems. It is surrounded equatorially by two strongly bound bidentate cppd molecules and axially by two weakly bound water molecules (Table 1). The bonds to the chelating cppd molecules, which are effectively coplanar with the CuN_4 equatorial plane (maximum displacement from the least-squares mean plane 0.093 Å), are almost identical in length (Table 1), despite the fact that the ligating nitrogens are in five- and six-membered aromatic rings. Centrosymmetrically related pairs of nitrate anions bridge the cations by hydrogen bonding to co-ordinated water molecules (Fig. 1, Table 2). The anions lie in the gap between the cations subtending a small dihedral angle (23.3°) to the CuN_4 equatorial plane.

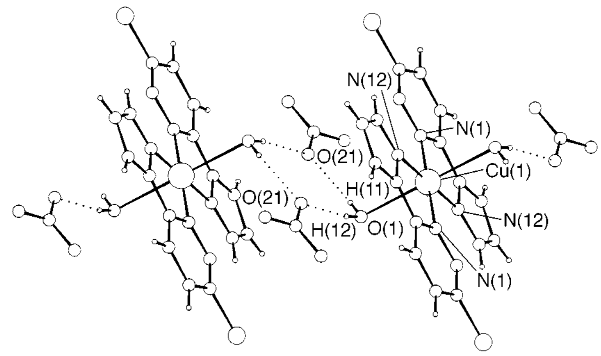

Fig. 1 Molecular structure and numbering scheme for complex **6** showing the centrosymmetric hydrogen-bonding interactions between $[Cu(cppd)_2(H_2O)_2]^{2+}$ cations and nitrate anions

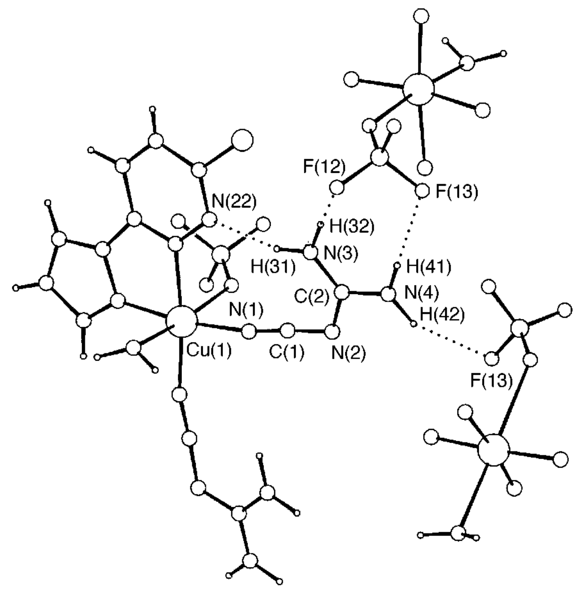

Fig. 2 Molecular structure and numbering scheme for $[Cu(cppd)(cnge)_2(H_2O)(FBF_3)][BF_4]$ **7** showing the intramolecular hydrogen-bonding interaction between the co-ordinated cnge (cnge 1) and cppd ligands and the intermolecular hydrogen-bonding interactions involving cnge 1

Crystal and molecular structure of complex 7

The copper atom in complex **7** (Figs. 2 and 3) is surrounded equatorially by a bidentate cppd ligand and two monodentate cnge molecules and axially by one water molecule and one BF_4^- anion. The equatorially located ligands are effectively coplanar with maximum deviations from the least-squares best planes of 0.017 Å (cnge 1), 0.072 Å (cnge 11) and 0.047 Å (cppd) and dihedral angles between the ligands and the equatorial plane of 14.1 (cnge 1), 12.7 (cnge 11) and 4.4° (cppd). The Cu–N distances are, however, quite asymmetric. In contrast to the situation in **6**, the bonds to the chelating cppd ligand differ by ≈0.1 Å (Table 1), that to the pyridazine ring nitrogen being considerably longer than that to the pyrazole ring nitrogen. The binding of the two cnge molecules is also asymmetric, that [N(1)] *trans*

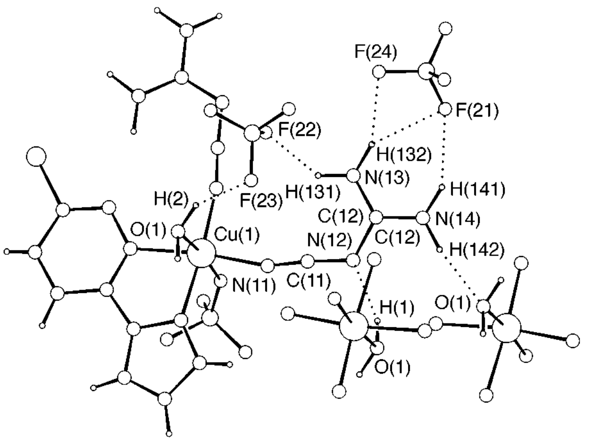

Fig. 3 Molecular structure and numbering scheme for complex **7** showing the intermolecular hydrogen-bonding interactions involving cnge 11

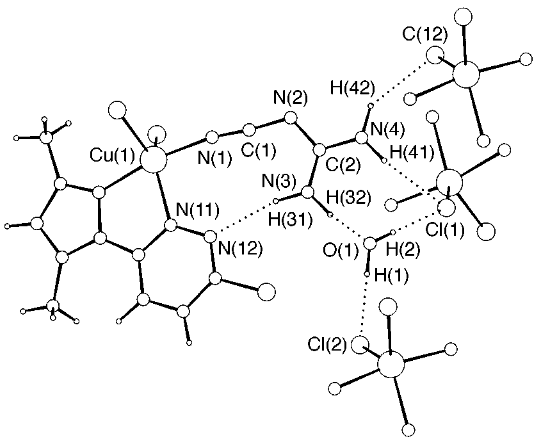

Fig. 4 Molecular structure and numbering scheme for [Cu(cmppd)(cnge)Cl_2]·H_2O **12** showing the intra- and inter-molecular hydrogen-bonding interactions

to the pyrazole nitrogen being more strongly bound than that [N(11)] *trans* to the pyridazine nitrogen (Table 1). These differences are manifest in the IR spectrum of the complex (Table 3) which shows four bands in the ν_{asym}(NCN) stretching region rather than the usual doublet.[6] The axial ligands are weakly co-ordinated, the water oxygen being somewhat closer to the copper atom than the tetrafluoroborate fluorine (Table 1), which is close to the limit of semico-ordination.[7,8] The coplanarity of the equatorially located ligands is enhanced by the formation of an intramolecular hydrogen bond between a cnge amino moiety and the pyridazine unco-ordinated nitrogen [N(3)–H(31) · · · N(22), Table 2]. Of the cnge ligands, the intramolecularly hydrogen-bonded one is the more strongly co-ordinated as evidenced by the shorter Cu–N interatomic distance and smaller deviation from linearity of the Cu–N–C co-ordinate angle (Table 1). The asymmetry of the chelating ligand co-ordination can also be related to these differences in *trans*-located cnge co-ordination.

The two cnge molecules are involved in a complex intermolecular hydrogen-bonding network with the axial ligands and the unco-ordinated $B(2)F_4^-$ anion (Table 2, Figs. 2 and 3). A detailed discussion is deferred to the section on guanidine hydrogen-bonding interactions.

The geometry of the co-ordinated $B(1)F_4^-$ anion does not reflect the involvement of the fluorines in intermolecular interactions. The B–F bonds, which are expected to decrease from B–F(11) (ligating fluorine) through B–F(12) and B–F(13) (hydrogen-bonded fluorines) to B–F(14) (uninvolved fluorine),[3] actually decrease in the order B–F(13) 1.412(8) > B–F(11) 1.372(8) > B–F(14) 1.369(8) > B–F(12) 1.364(8). The average B–F distance (1.379 Å), however, is similar to that in other co-ordinated BF_4^- anions (*e.g.* 1.365 Å in **3**[2]). The detailed structure of the unco-ordinated $B(2)F_4^-$ anion in **7** cannot be similarly analysed owing to its disorder. The IR spectrum of **7** is consistent with symmetrical anions and hence a weak Cu · · · F interaction, splitting of the triply degenerate ν(B–F) mode (T_2) of BF_4^- {centred at 1050 cm^{-1}} not being observed.[9]

Crystal and molecular structures of complex 12

The trigonal-bipyramidal copper co-ordination sphere in complex **12** (Fig. 4) comprises two equatorial chlorine atoms, an axial cnge molecule and a bidentate cmppd ligand which straddles axial and equatorial sites. As for **7**, the pyridazine nitrogen in **12** is further from the copper atom than is the pyrazole nitrogen (Table 1). In this case, however, the former occupies the weakly binding equatorial site and the latter the more strongly binding axial site (Table 1). This arrangement facilitates the formation of an intramolecular hydrogen bond between a cnge amino moiety and the pyridazine unco-ordinated nitrogen [N(3)–H(31) · · · N(12), Table 2]. To promote this interaction, the cnge and cmppd molecules are effectively coplanar and perpendicular to the copper(II) equatorial plane with maximum deviations from the least-squares best planes of 0.009 (cnge) and 0.167 Å (cmppd) and dihedral angles of 13.1 (cnge–cmppd), 83.2 (cnge-equatorial) and 83.7° (cmppd-equatorial). The copper atom is located 0.13 Å above the equatorial plane in the direction of the cnge molecule. The co-ordinate angle of the cnge molecule (Cu–N–C 170.0°) is almost identical to that (169.5°) of the intramolecularly hydrogen-bonded cnge molecule in **7**, as are the structural parameters of the corresponding hydrogen-bond contacts (N · · · N 3.19, H · · · N 1.0, 2.21 Å, N–H–N 165° **7**; N · · · N 3.24, H · · · N 1.0, 2.26 Å, N–H–N 167° **12**).

The cnge molecule is involved in a complex intermolecular hydrogen-bonding network with the unco-ordinated water molecule and chloride anions of adjacent complexes (Table 2, Fig. 4). A detailed discussion is deferred to the section on guanidine hydrogen-bonding interactions.

Crystal and molecular structures of complex 11

The trigonal-bipyramidal copper atom in complex **11** is surrounded by two chelating cmppd molecules and a single monodentate cnge ligand (Fig. 5). As in **12**, each cmppd occupies one axial and one equatorial position, with the pyrazole nitrogens in the strongly binding axial and the pyridazine nitrogens in the weakly binding equatorial sites (Table 1). The equatorial located cnge molecule is closer to the copper atom than the pyridazine nitrogens owing to the difference in the N(sp) and N(sp^2) radii (Table 1). The three ligands are effectively planar with maximum displacements from the least-squares mean planes of 0.098 (cnge), 0.101 (cmppd 11) and 0.159 Å (cmppd 31). The copper atom is only marginally displaced (0.022 Å) from the equatorial plane and is equidistant from the two axial pyrazole nitrogens. The dihedral angles between the ligands and the equatorial plane are 42.1 (cnge), 87.4 (cmppd 11) and 81.6° (cmppd 31). This co-ordination geometry precludes coplanarity of the cnge and cmppd ligands and hence the formation of an intramolecular hydrogen bond as found in **12**. The co-ordinate angle of the cnge molecule (Cu–N–C 164.2°) is comparable with that (146.0°) of the cnge molecule in **5**, the structurally analogous 2,2′-bipy complex.

All four N–H moieties of the cnge molecule are involved in an intermolecular hydrogen-bonding network with the two anions (Table 2, Fig. 5), neither of which is disordered. A double N–H donor interaction locates $B(1)F_4^-$ and single N–H · · · F contacts hold $B(2)F_4^-$ in a bridging position (Fig. 5) generating a chain parallel to the *a* axis. The only contacts between chains involve van der Waals or electrostatic interactions. The geometries of the anions [B(1)–F 1.36(1)–1.40(1), average 1.39; B(2)–F 1.356(8)–1.421(8), average 1.39 Å] and IR

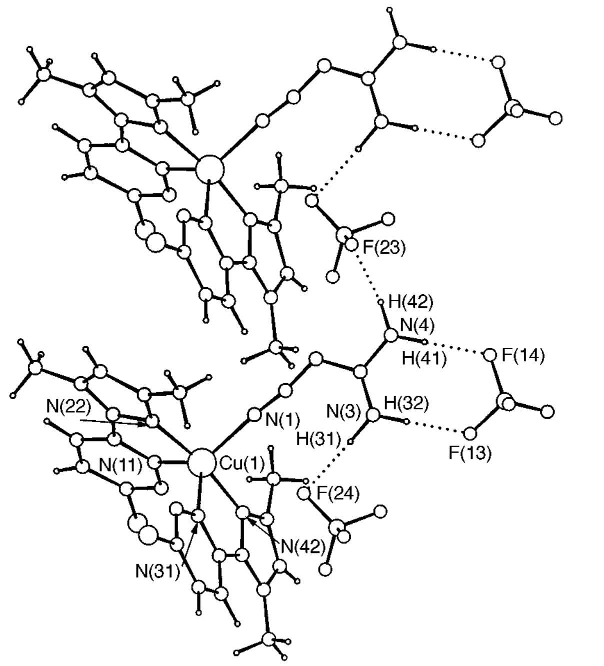

Fig. 5 Molecular structure and numbering scheme for $[Cu(cmppd)_2(cnge)][BF_4]_2$ **11** showing the intermolecular hydrogen-bonding interactions

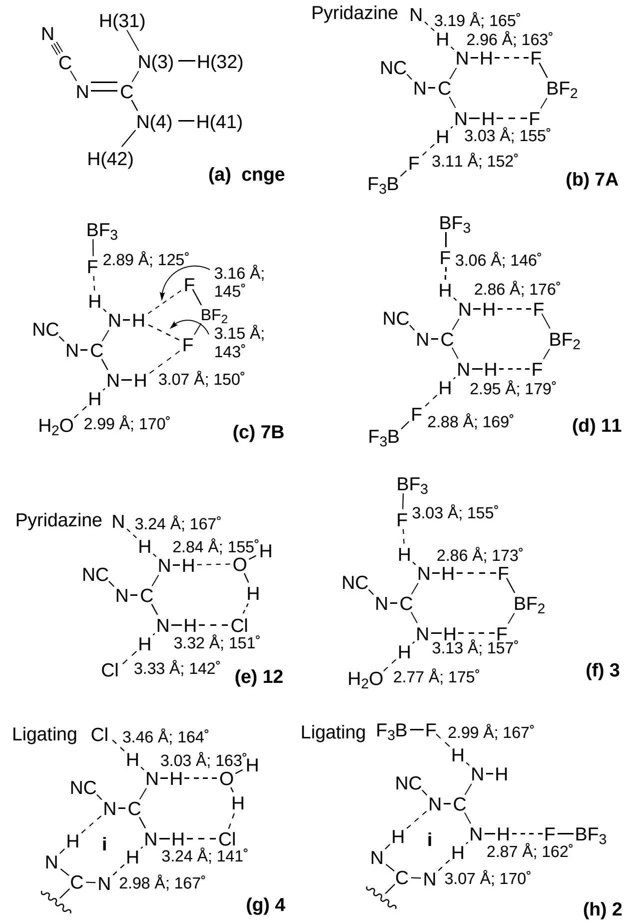

Scheme 3 2-Cyanoguanidine numbering scheme (a) and hydrogen-bonding interactions in (b, c) $[Cu(cppd)(cnge)_2(H_2O)(FBF_3)[BF_4]$ **7A**, **7B**, (d) $[Cu(cmppd)_2(cnge)][BF_4]_2$ **11**, (e) $[Cu(cmppd)(cnge)Cl_2]$ **12**, (f) $[Cu(2,2'\text{-bipy})_2(cnge)][BF_4]_2$ **3**, (g) $[Cu(2,2'\text{-bipy})(cnge)Cl_2]$ **4**, and (h) $[Cu(2,2'\text{-bipy})(cnge)_2(FBF_3)_2]$ **2**

spectrum of **11** are consistent with isolated BF_4^- units. A more detailed discussion of the hydrogen-bonding interactions is deferred to the section on guanidine hydrogen-bonding interactions.

Crystal structure of complex 9

Oscillation and Weissenberg photographs, together with density measurements (flotation in bromoform–hexane mixtures), for complex **9** revealed a monoclinic unit cell with $P2_1/c$ symmetry and $Z = 2$, thus locating the copper atom of an inversion centre. By analogy with **6**, which has a very similar electronic spectrum to that of **9**, the two cppd ligands will occupy equatorial sites and water molecules the axial sites with lattice bromide. However, the alternative axial location of bromide anions with lattice water cannot be discounted as the weakly bound axial ligand will have marginal effect on the electronic structure and spectra of the complexes. The identical stoichiometry and similar spectroscopic properties of **8** to **6** and **9** suggest it too adopts a similar structure.

Infrared spectroscopic diagnosis of cnge co-ordination

Selected IR data for the products are quoted in Table 3; they confirm the presence of cnge, cppd or cmppd, and NO_3^- or BF_4^-, as appropriate. Those for the anions are consistent with D_{3h} (NO_3^-) or T_d (BF_4^-) symmetry. Co-ordination of cppd and cmppd is confirmed by the shifting of the 1455 and 1425 cm^{-1} bands, respectively, to higher frequency.

The ν_{asym}(NCN) 'doublet' in the IR spectrum of cnge (2209/2165 cm^{-1}), which shifts when co-ordinated to transition metals, is helpful in structure elucidation. For most complexes it moves to higher frequency,[6,10] following a similar pattern to that of co-ordinated cyanide,[9] and shows a reversal in the relative intensities of the two bands. Complex **12**, in which the cnge molecule is located in a strongly bonding axial site of a trigonal-bipyramidal co-ordination sphere, is a typical example. For a very limited number of complexes the relative intensities of the two bands are the same as for free cnge. Complex **11**, in which the cnge molecule is located in a weakly bonding equatorial site of a trigonal-bipyramidal co-ordination sphere, is a typical example.

This region of the IR spectra of complexes **10** and **13** can be used, together with UV/VIS spectral data, to probe their structural chemistry. The spectra of **10** compare with those for **7**, which has the same 2 : 1 diimine : cnge ratio, and the spectra for **13** are analogous to those for **12**, which has the same stoichiometry. The IR spectra of **7** and **10** contain two ν_{asym}(NCN) doublets (all other absorptions attributable to cnge are also split into two bands). The two doublets are undoubtedly due to the presence of two crystallographically independent cnge molecules (Fig. 2). The higher-frequency doublet is assigned to the intramolecularly hydrogen-bonded ligand by comparison with the spectral data for **12**.

Guanidine hydrogen-bonding interactions; comparison with copper(II)–2,2′-bipy–cnge complexes

The hydrogen-bonding sequences formed by the guanidine functions of the co-ordinated cnge molecules exhibit consistent patterns. Those in complex **7** (the crystallographically independent cnge molecules are designated **7A** and **7B**), **11** and **12** are shown in Scheme 3 together with those for the corresponding copper(II)–cnge-2,2′-bipy complexes, **2**, **3** and **4**. For ease of comparison, the cnge numbering sequence is the same in all complexes [Scheme 3(a)]. Given the choice postulated in Scheme 1, intramolecular N(3)–H(31) · · · X hydrogen bonds are formed in **7** [**7A**, Scheme 3(b)] and **12** [Scheme 3(e)] to the non-ligating pyridazine nitrogen, not the anion. In the absence of the pyridazine nitrogen, which is presumed to be a more effective hydrogen-bond acceptor than the anions, N(3)–H(31) · · · anion hydrogen bonds are formed as in the 2,2′-bipy complexes **2** [Scheme 3(h)] and **4** [Scheme 3(g)]. Intramolecular cnge–cppd (or cmppd) contacts only occur when the two

Table 1 Interatomic distances (Å) and angles (°) in the copper co-ordination spheres of $[Cu(cppd)_2(H_2O)_2][NO_3]_2$ **6**, $[Cu(cppd)(cnge)_2(H_2O)(FBF_3)][BF_4]$ **7**, $[Cu(cmppd)_2(cnge)][BF_4]_2$ **11** and $[Cu(cmppd)(cnge)Cl_2]\cdot H_2O$ **12**

Pyridazine nitrogen	**6** N(1)	1.996(2)	**7** N(21)	2.056(5)	**11** N(11)	2.070(5)	**11** N(31)	2.052(5)	**12** N(11)	2.105(2)
Pyrazole nitrogen	**6** N(12)	1.998(2)	**7** N(32)	1.957(4)	**11** N(22)	1.965(5)	**11** N(42)	1.965(5)	**12** N(22)	1.959(2)
Nitrile nitrogen	**7** N(1)	1.908(4)	**7** N(11)	1.966(5)	**11** N(1)	2.007(6)			**12** N(1)	1.927(2)
Additional ligands	**6** O(1)	2.410(3)	**7** O(1)	2.449(4)	**7** F(11)	2.726(5)	**12** Cl(1)	2.3976(7)	**12** Cl(2)	2.3621(7)

Complex **6**							
N(1)–Cu–N(12)	80.0(1)	N(1)–Cu–O(1)	87.2(1)	N(12)–Cu–O(1)	89.1(1)		
Complex **7**							
N(1)–Cu–N(11)	92.7(2)	N(1)–Cu–N(21)	94.6(2)	N(1)–Cu–N(32)	170.9(2)		
N(1)–Cu–O(1)	93.7(2)	N(1)–Cu–F(11)	89.2(2)	N(11)–Cu–N(21)	172.7(2)		
N(11)–Cu–N(32)	93.8(2)	N(11)–Cu–O(1)	90.1(2)	N(11)–Cu–F(11)	93.2(2)		
N(21)–Cu–N(32)	79.0(2)	N(21)–Cu–O(1)	89.5(2)	N(21)–Cu–F(11)	86.8(2)		
N(32)–Cu–O(1)	92.7(2)	N(32)–Cu–F(11)	84.1(2)	O(1)–Cu–F(11)	175.5(2)		
Complex **11**							
N(1)–Cu–N(11)	121.7(2)	N(1)–Cu–N(22)	95.2(2)	N(1)–Cu–N(31)	119.1(2)		
N(1)–Cu–N(42)	94.9(2)	N(11)–Cu–N(22)	78.1(2)	N(11)–Cu–N(31)	119.2(2)		
N(11)–Cu–N(42)	94.9(2)	N(22)–Cu–N(31)	98.7(2)	N(22)–Cu–N(42)	169.5(2)		
N(31)–Cu–N(42)	77.7(2)						
Complex **12**							
N(1)–Cu–N(11)	92.84(8)	N(1)–Cu–N(22)	170.30(9)	N(1)–Cu–Cl(1)	92.32(7)		
N(1)–Cu–Cl(2)	95.00(7)	N(11)–Cu–N(22)	77.76(8)	N(11)–Cu–Cl(1)	121.77(6)		
N(11)–Cu–Cl(2)	122.48(6)	N(22)–Cu–Cl(1)	90.64(6)	N(22)–Cu–Cl(2)	92.15(6)		
Cl(1)–Cu–Cl(2)	114.72(3)						
cnge co-ordinate angles							
7		**11**		**12**			
Cu–N(1)–C(1)	169.5(5)	Cu–N(1)–C(1)	164.2(5)	Cu–N(1)–C(1)	170.0(2)		
Cu–N(11)–C(11)	162.9(5)						
Diimine co-ordinate angles							
Complex **6**							
Cu–N(1)–N(2)	122.1(2)	Cu–N(1)–C(6)	116.1(2)	Cu–N(12)–N(11)	112.0(2)	Cu–N(12)–C(13)	142.8(2)
Complex **7**							
Cu–N(21)–N(22)	123.9(3)	Cu–N(21)–C(26)	114.6(4)	Cu–N(32)–N(31)	114.9(4)	Cu–N(32)–C(33)	139.4(5)
Cu–F(11)–B(1)	139.4(4)						
Complex **11**							
Cu–N(11)–N(12)	121.6(4)	Cu–N(11)–C(16)	115.6(4)	Cu–N(22)–N(21)	116.7(4)	Cu–N(22)–C(23)	137.7(5)
Cu–N(31)–N(32)	121.8(4)	Cu–N(31)–C(36)	117.2(4)	Cu–N(42)–N(43)	115.7(4)	Cu–N(42)–C(46)	136.8(5)
Complex **12**							
Cu–N(11)–N(12)	124.1(2)	Cu–N(11)–C(16)	114.8(2)	Cu–N(22)–N(21)	116.5(1)	Cu–N(22)–C(23)	136.4(2)

ligands are coplanar and *cis* located with 90° interligand angles, as in **7** and **12**. When coplanarity is impossible, as in **11** (the second cmppd molecule would have to straddle two equatorially located sites with an N–Cu–N angle of ≈120°), N(3)–H(31) is involved in a bent intermolecular contact to an anion [Scheme 3(d)]. A similar arrangement occurs in the 2,2′-bipy analogue **3** [Scheme 3(f)] as well as for the second cnge molecule in **7** [**7B**, Scheme 3(c)].

With unco-ordinated BF_4^- anions the favoured interaction for the N(3)–H(32) and N(4)–H(41) moieties is a double contact as for complexes **7A**, **11** and **3** [Scheme 3(b), (d) and (f)]. When the BF_4^- anion is not involved in any other contacts, as in **11**, the hydrogen bonds are relatively short and almost linear. Involvement of the anion in other interactions leads, depending on their magnitude, to either lengthening and bending of the hydrogen bonds as for **7A** and **3** or bifurcation as for **7B** [Scheme 3(c)]. Double contacts of this type are commonplace in cnge structural chemistry.[11–13] Since they occur with not only BF_4^- [11,12] but also NO_3^-,[13] which have sp^3 and sp^2 angles respectively, a degree of flexibility must pertain.

The N(3)–H(32) and N(4)–H(41) moieties are also involved in analogous structural motifs in the two chloro complexes, **12** and **4** [Scheme 3(e) and (g)]. Eight-membered hydrogen-bonded rings are formed as in the BF_4^- complexes, **7**, **11** and **3**, but with an ···O–H···Cl··· contact replacing the ···F–BF_2–F··· link.

In the cppd or cmppd complexes the fourth amine function on the guanidine moiety, N(4)–H(42), is variously bonded to anions or water molecules. In the 2,2′-bipy complexes, **2** and **4**, however, it is involved in the formation of a centrosymmetric paired donor acceptor N(4)–H(42)···N(2) contact [Scheme 3(g) and (h)]. Such interactions are frequently observed in cnge structural chemistry.[10,11]

Copper co-ordination geometries; comparison with copper(II)–2,2′-bipy–cnge complexes

The co-ordination geometries in the two sets of mixed-ligand complexes are compared in Scheme 4. They fall into three pairs: **7** and **2** [Scheme 4(a) and (b)], **12** and **4** [4(c) and (d)], **11** and **3** [4(e) and (f)]. The incorporation of a hydrogen-bonding acceptor site in the bidentate chelating ligand radically alters the intramolecular contacts; cnge–anion hydrogen bonds in **2** and **4** are replaced by cnge–pyridazine interactions in **7** and **12**.

Table 2 Hydrogen-bonding interactions (distances/Å and angles/°) in complexes **6**, **7**, **11** and **12**

Interaction X–H···X′	Symmetry of X′	X–H	X···X′	H···X′	X–H···X′
Complex **6**					
O(1)–H(11)···O(21)	$-x, 1-y, 1-z$	0.72(4)	2.877(4)	2.18(4)	164(4)
O(1)–H(12)···O(21)	x, y, z	0.78(5)	2.838(4)	2.08(5)	168(4)
Complex **7**					
O(1)–H(1)···N(12)	$1-x, -y, -z$	0.97	2.924(6)	2.01	157
O(1)–H(2)···F(23)	x, y, z	0.90	2.829(7)	2.07	142
N(3)–H(31)···N(22)	x, y, z	1.00	3.189(7)	2.21	165
N(3)–H(32)···F(12)	$-x, 1-y, -z$	1.00	2.960(7)	1.99	163
N(4)–H(41)···F(13)	$-x, 1-y, -z$	1.00	3.029(7)	2.09	155
N(4)–H(42)···F(13)	$-0.5+x, 0.5-y, -0.5+z$	1.00	3.107(7)	2.19	152
N(13)–H(131)···F(22)	x, y, z	1.00	2.890(10)	2.20	125
N(13)–H(132)···F(21)	$0.5-x, -0.5+y, -0.5-z$	1.00	3.163(8)	2.29	145
N(13)–H(132)···F(24)	$0.5-x, -0.5+y, -0.5-z$	1.00	3.150(8)	2.29	143
N(14)–H(141)···F(21)	$0.5-x, -0.5+y, -0.5-z$	1.00	3.067(7)	2.16	150
N(14)–H(142)···O(1)	$x, -1+y, z$	1.00	2.988(7)	2.00	170
Complex **11**					
N(3)–H(31)···F(24)	x, y, z	1.00	3.058(7)	2.18	146
N(3)–H(32)···F(13)	$-0.5+x, -0.5+y, z$	1.00	2.863(8)	1.87	176
N(4)–H(41)···F(14)	$-0.5+x, -0.5+y, z$	1.00	2.952(8)	1.95	179
N(4)–H(42)···F(23)	$-1+x, y, z$	1.00	2.875(7)	1.89	169
Complex **12**					
N(3)–H(31)···N(12)	x, y, z	1.00	3.238(3)	2.26	167
N(3)–H(32)···O(1)	x, y, z	1.00	2.841(3)	1.90	155
N(4)–H(41)···Cl(1)	$1-x, -y, 1-z$	1.00	3.320(2)	2.41	151
N(4)–H(42)···Cl(2)	$0.5+x, 0.5-y, 0.5+z$	1.00	3.330(2)	2.49	142
O(1)–H(1)···Cl(2)	$-0.5+x, 0.5-y, 0.5+z$	0.94	3.123(2)	2.19	179
O(1)–H(2)···Cl(1)	$1-x, -y, 1-z$	0.93	3.089(2)	2.16	179

Angles at O(1): Cl(1)–O(1)–Cl(2) 121.46(7), Cl(1)–O(1)–N(3) 91.01(8), Cl(2)–O(1)–N(3) 124.38(8); average 112.28.

Table 3 Reaction stoichiometries, product analyses and IR spectroscopic data

	Reagents											
	Copper salt[b]		L		cnge		Product yield			Product analysis (%)[a]		
Complex	g	mmol	g	mmol	g	mmol	g	mmol	%	C	H	N
6	1.60	6.62	0.40	2.21	0.37	4.40	0.12	0.21	19	28.25 (28.75)	2.40 (2.40)	23.70 (23.95)
7	1.45	4.86	0.41	2.27	0.33	3.92	0.60	0.96	49	21.15 (21.90)	2.40 (2.50)	26.70 (27.85)
8	0.57	3.32	0.20	1.11	0.19	2.21	0.08	0.15	27	31.25 (31.65)	2.50 (2.65)	20.90 (21.10)
9	0.48	2.15	0.13	0.72	0.12	1.44	0.31	0.50	69	27.15 (27.10)	2.25 (2.25)	18.50 (18.05)
10	1.42	5.88	0.42	2.01	0.33	3.92	0.55	0.78	40	22.95 (23.20)	2.90 (4.35)	29.80 (29.15)
11	1.46	4.89	0.36	1.73	0.34	4.04	0.60	0.81	94	31.55 (32.55)	2.90 (3.00)	22.00 (22.75)
12	0.83	4.87	0.43	2.06	0.34	4.04	0.83	1.86	90	29.60 (29.70)	3.35 (3.40)	24.70 (25.15)
13	0.38	1.70	0.12	0.57	0.10	1.14	0.27	0.51	89	24.20 (24.65)	2.40 (2.85)	20.85 (20.90)

IR spectral data/cm^{-1}

	cnge		cppd/cmppd					Anion
cnge	2209m	2165s						
cppd			1455s	1407s	1149s	863m	764s	
6	—	—	1473s	—	1170s	854m	786s	1383s
7	2253/35s	2206/2192m	1474m	1409m	—	846w	783w	1050s (br)
8	—	—	1473s	1408s	1173m	861w	793m	
9	—	—	1473s	1408s	1170m	855m	786m	
cmppd			1425s	1364m	1085s	854m	792m	
10	2243/20s	2201/2176m	1430s	—	—	829w	800w	1384s (br)
11	2235m	2189s	1427s	—	—	841w	802w	1084s (br)
12	2254s	2202w	1430s	1376w	1070m	827m	797m	
13	2256s	2200m	1429s	1376w	1068m	824m	796m	—

[a] Calculated value in parentheses. [b] $Cu(NO_3)_2·3H_2O$ for complexes **6** and **10**, $Cu(BF_4)_2·3.4H_2O$ for **7** and **11**, $CuCl_2·2H_2O$ for **8** and **12**, $CuBr_2$ for **9** and **13**.

Thus, although intramolecular N–H···F interactions support the co-ordination of the axially located tetrafluoroborate anion in **2** [Scheme 4(b)],[2] the corresponding amino group in **7** forms a strong N–H···N contact to the pyridazine unco-ordinated nitrogen [4(a)]. The absence of intramolecular ligand–anion hydrogen-bonding interactions (Table 2, Fig. 2) is reflected in the positions of the co-ordinated anion, Cu···F in **7** (2.726 Å) being considerably longer than in **2** (2.526 Å).[2]

To accommodate the incorporation of a N–H···N contact in complex **12** at the expense of an intramolecular N–H···Cl

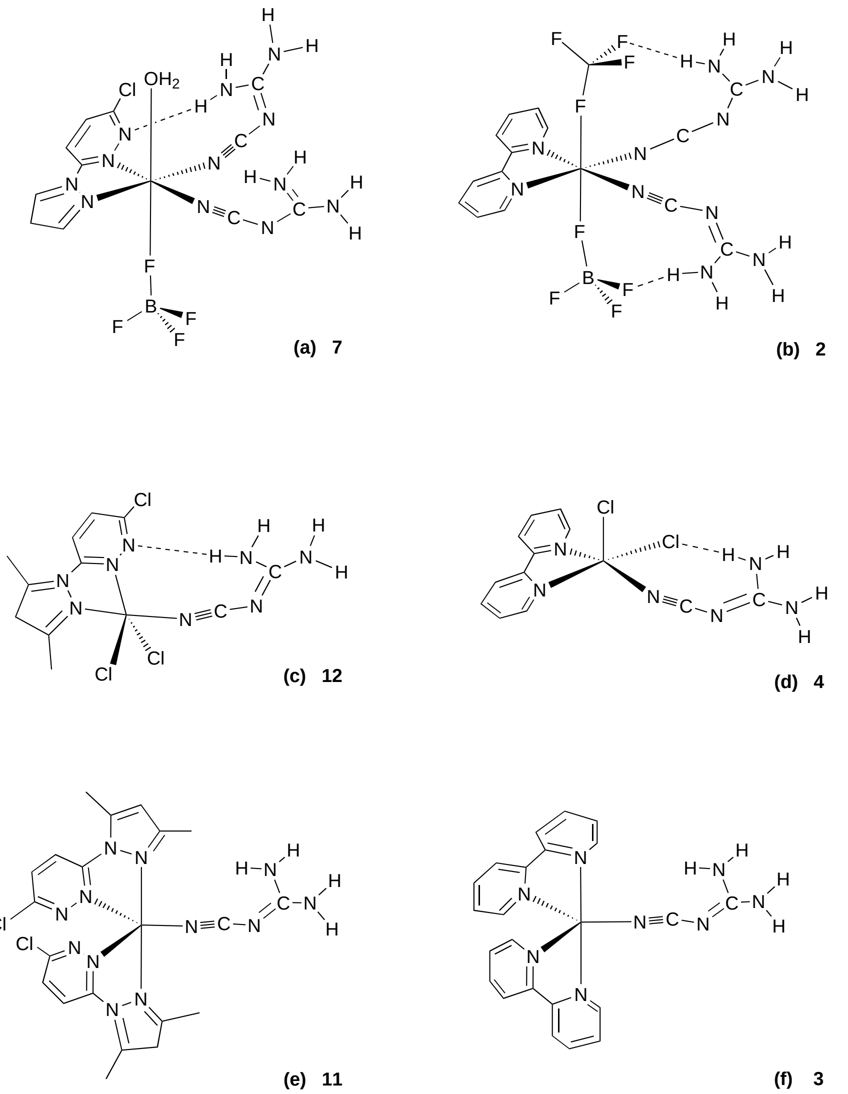

Scheme 4 Comparison of the copper(II) co-ordination geometries in (a) $[Cu(cppd)(cnge)_2(H_2O)(FBF_3)]^+$ **7**, (b) $[Cu(2,2'\text{-bipy})(cnge)_2(FBF_3)_2]$ **2**, (c) $[Cu(cmppd)(cnge)Cl_2]$ **12**, (d) $[Cu(2,2'\text{-bipy})(cnge)Cl_2]$ **4**, (e) $[Cu(cmppd)_2(cnge)]^{2+}$ **11**, and (f) $[Cu(2,2'\text{-bipy})_2(cnge)]^{2+}$ **3**

contact as in **4**,[2] whilst retaining the same molecular formula, the copper co-ordination geometry changes from square-based pyramidal in **4** [Scheme 4(d); cnge equatorial, chloride axial][2] to trigonal bipyramidal in **12** [Scheme 4(c); cnge axial, cmppd equatorial).

The only pair of complexes with near-identical co-ordination geometries are the $[Cu(diimine)_2(cnge)]^+$ cations (diimine = 2,2′-bipy or cmppd) in **11** and **3**[2] which do not exhibit any intramolecular hydrogen bonds [Scheme 4(e) and (f)].

Conclusion

With the exception of **7**, mixed-ligand complexes are not formed by cppd. We attribute this to the stability of the centrosymmetric tetragonally elongated octahedral geometries of the bis(cppd) complexes, **6** (Fig. 1), **8** and **9**. The compound cmppd does not form complexes analogous to **6**, **8** and **9** with coplanar chelating ligands presumably owing to steric hindrance caused by the methyl group in the 3 position of the pyrazole ring. Similarly, bis(diimine)copper(II) complexes [diimine = 2,2′-bipy, 1,10-phenanthroline or bis(pyrid-2-yl)amine] do not form analogous complexes to **6**, **8** and **9**. Instead, either (in the absence of co-ordinating anions[8,14]) compressed tetrahedral CuN_4 chromophores with 40–60° dihedral angles between chelating ligands or (in the presence of co-ordinating anions[15]) trigonal-bipyramidal stereochemistries similar to those of **3** and **11** are formed. Steric repulsion between the hydrogens in the α positions of the pyridine rings must be responsible for the distorted and less stable structures of these $[Cu(diimine)_2]^{2+}$ complexes.[8,14] The absence of complexes structurally analogous to **6**, **8** and **9** for cmppd and 2,2′-bipy rationalises the facile formation of mixed-ligand complexes **1**–**5** and **10**–**13**.

In both structurally characterised cmppd complexes, **11** and **12**, the diimine straddles equatorial–axial positions of trigonal-bipyramidal co-ordination spheres with cnge located either equatorially (**11**) or axially (**12**). All three diimines are arranged such that the pyridazine nitrogens occupy the equatorial sites and the pyrazole nitrogens the more strongly co-ordinating axial sites. For the two complexes for which structural data are not available, spectroscopic evidence indicates that the structure of **13** is the same as that of **12** and that the structure of **10** is analogous to that of **7**.

The guanidine hydrogen-bonding interactions follow consistent patterns; N(3)–H(31) is involved in intramolecular contacts to either the non-ligating pyridazine nitrogen (cppd or cmppd complexes) or co-ordinated anion (2,2′-bipy complexes), N(3)–H(32) and N(4)–H(41) form double N–H···F contacts with BF_4^- and N(4)–H(42) is involved in centrosymmetric paired donor–acceptor N(4)–H(42)···N(2) contacts.

Experimental

All reagents (Aldrich Chemical Company Ltd.) were used as received, apart from cnge which was recrystallised from hot deionised water prior to use. Elemental analysis (C, H, N) was performed using a Perkin-Elmer 240B Elemental Analyser by

Table 4 Crystallographic data for $[Cu(cppd)_2(H_2O)_2][NO_3]$ **6**, $[Cu(cppd)(cnge)_2(H_2O)(FBF_3)][BF_4]$ **7**, $[Cu(cmppd)_2(cnge)][BF_4]_2$ **11** and $[Cu(cmppd)(cnge)Cl_2]\cdot H_2O$ **12**

Complex	**6**	**7**	**11**	**12**
Formula	$C_{14}H_{14}Cl_2CuN_{10}O_8$	$C_{11}H_{15}B_2ClCuF_8N_{12}O$	$C_{20}H_{22}B_2Cl_2CuF_8N_{12}$	$C_{11}H_{15}Cl_3CuN_8O$
M	584.78	603.92	738.53	445.19
Space group (monoclinic)	$P2_1/c$ (no. 14)	$P2_1/n$ (no. 14)	*Cc* (no. 9)	$P2_1/n$ (no. 14)
a/Å	6.867(4)	12.436(2)	8.785(2)	9.224(3)
b/Å	7.629(4)	8.754(3)	23.901(6)	10.518(2)
c/Å	20.954(12)	20.932(5)	14.984(4)	17.850(4)
β/°	98.52(5)	103.096(14)	105.96(2)	94.07(6)
Z	2	4	4	4
$U/Å^3$	1085.6(11)	2219.4(7)	3025.1(10)	1727.5(8)
μ/mm^{-1}	1.319	1.199	0.983	1.752
$D_c/g\ cm^{-3}$	1.789	1.807	1.622	1.712
$D_m/g\ cm^{-3}$ (bromoform–hexanes)	—	1.80	1.59	1.70
F(000)	590	1206	1486	900
Crystal dimensions/mm	0.16 × 0.25 × 0.33	0.12 × 0.29 × 0.42	0.28 × 0.26 × 0.24	0.37 × 0.35 × 0.31
T/K	150	220	150	150
Index ranges	$-8 \le h \le 8$, $0 \le k \le 9$, $0 \le l \le 24$	$-14 \le h \le 14$, $0 \le k \le 10$, $0 \le l \le 24$	$-10 \le h \le 10$, $0 \le k \le 28$, $-17 \le l \le 17$	$-10 \le h \le 10$, $0 \le k \le 12$, $0 \le l \le 21$
Reflections collected	2065	4182	3665	4691
Independent reflections	1758	3493	3488	2916
Reflections with $I > 2\sigma(I)$	1578	2891	3171	2638
Data, restraints, parameters	1758, 0, 188	3493, 0, 341	3488, 0, 407	2916, 0, 217
R, *R′* (all data)	0.0465, 0.0273	0.0824, 0.1037	0.0679, 0.0826	0.0360, 0.0457
[data with $I \ge 2\sigma(I)$]	0.0388, 0.0253	0.0662, 0.0853	0.0621, 0.0786	0.0309, 0.0424
ρ_{min}, $\rho_{max}/e\ Å^{-3}$	−0.418, 0.45	−0.666, 1.159	−0.77, 1.36	−0.42, 0.62
$(\Delta/\sigma)_{max}$ in final cycle	0.04	0.01	0.02	0.02

Common parameters: Mo-Kα radiation (λ = 0.710 73 Å); $2\theta_{max} = 50°$.

Mr. T. Spencer of the Nottingham University Chemistry Department Analytical Services Group. Magnetic susceptibility data were determined using the Gouy-balance method. Infrared spectra, in KBr discs or as Nujol mulls between KBr windows, UV/VIS spectra, in aqueous solution [(1–10) × 10^{-4} mol dm^{-3}] and ^1H NMR spectra ($CDCl_3$) were recorded using Perkin-Elmer 983G, Unicam UV2-100 and Brücker 300 MHz spectrometers, respectively.

Preparation of ligands

3-Chloro-6-(pyrazol-1-yl)pyridazine. Pyrazole (2.0 g, 0.029 mol) was dissolved in dry tetrahydrofuran (100 cm^3) and small pieces of clean potassium metal (1.149 g, 0.029 mol) were added with stirring under nitrogen to yield a white precipitate. An exit needle was fitted to the reaction vessel to permit hydrogen release. Upon complete reaction (12 h), a solution of 3,6-dichloropyridazine (8.641 g, 0.058 mol) in dry tetrahydrofuran (50 cm^3) was added with stirring to yield a red-brown solution which was refluxed for 4 h. After cooling, the resulting red-brown suspension was added to ice-cold deionised water (250 cm^3) to yield a white precipitate which was filtered off under suction, washed with ice-cold deionised water and dried under vacuum over phosphorus pentaoxide to give cppd as a white powder. Yield 3.862 g (74%), m.p. 135–136 °C [Found (Calc. for $C_7H_5ClN_4$): C, 46.30 (46.55); H, 2.60 (2.80); N, 30.70 (31.00%)]. EI mass spectrum (*m*/*z*, relative intensity): 180 {M^+, $[(C_3H_3N_2)(C_4H_2ClN_2)]^+$, 100}, 153 {$[(C_2H_2N)(C_4H_2ClN_2)]^+$, 16}, 117 {$[(C_3H_3N_2)(C_4H_2)]^+$, 16}, 90 {$[(C_2H_2N)(C_4H_2)]^+$, 18}, 73 ($[C_3H_2Cl]^+$, 22), 64 ($[C_4H_2N]^+$, 15) and 52 ($[C_3H_2N]^+$, 16%). ^1H NMR ($CDCl_3$) : δ 8.73 (t, *J* 1.58, 1 H), 8.30 (d, *J* 9.17, 1 H), 8.20 (d, *J* 1.07, 1 H), 7.79 (d, *J* 9.24, 1 H) and 6.54 (dd, *J* 1.34 Hz, 1 H). IR (KBr disc): $\tilde{\nu}/cm^{-1}$ 3120m, 3066m, 2963m, 2925m, 2186m, 1654s, 1577s, 1526s, 1498m, 1455s, 1406s, 1385s, 1261m, 1148m, 1098m, 1053m, 1018m, 933w, 863m, 802m, 765m and 611m.

3-Chloro-6-(3,5-dimethylpyrazol-1-yl)pyridazine. This compound was prepared as for cppd using 3,5-dimethylpyrazole (4.005 g, 0.0417 mol) instead of pyrazole, potassium metal (1.629 g, 0.0417 mol) and 3,6-dichloropyridazine (9.289 g, 0.0624 mol). Yield 6.001 g (69%), m.p. 104–106 °C [Found (Calc. for $C_9H_9ClN_4$): C, 51.20 (51.80); H, 4.50 (4.35); N, 26.25 (26.85%)]. EI mass spectrum (*m*/*z*, relative intensity): 208 {M^+, $[(C_5H_7N_2)(C_4H_2ClN_2)]^+$, 100}, 191 {$[(C_4H_4N_2)(C_4H_2ClN_2)]^+$, 31}, 180 {$[(C_5H_7N_2)(C_4H_2Cl)]^+$, 18}, 173 {$[(C_5H_7N_2)(C_4H_2N_2)]^+$, 20}, 166 {$[(C_5H_7N)(C_4H_2Cl)]^+$, 7}, 129 {$[(N)(C_4H_2ClN_2)]^+$, 18}, 95 ($[C_5H_7N_2]^+$, 68), 81 ($[C_5H_7N]^+$, 36) and 73 ($[C_3H_2Cl]^+$, 62%). ^1H NMR ($CDCl_3$): δ 8.16 (d, *J* 9.30, 1 H), 7.56 (d, *J* 9.21 Hz, 1 H), 6.06 (s, 1 H), 2.72 (s, 3 H) and 2.29 (s, 3 H). IR (KBr disc): $\tilde{\nu}/cm^{-1}$ 3054m, 1576s, 1543m, 1425s, 1364m, 1270w, 1141m, 1066m, 1008w, 972m, 854m, 792m, 744m, 591w, 529w and 511m.

Preparation of complexes

The eight complexes were prepared by a protocol similar to that described previously for copper(II)–bipy–cnge systems.[2] Quantitative details for the experiments, together with analytical and IR spectroscopic data for the products, are given in Table 3. The magnetic susceptibility data for all eight complexes were consistent with mononuclear d^9 systems ($\mu = 1.7–1.9\ \mu_B$; $\mu_B \approx 9.27 \times 10^{-24}\ J\ T^{-1}$) and the UV/VIS spectra showed single broad bands centred close to 700 nm for **6**–**9** (blue), 725 nm for **10** (turquoise), 770 nm for **11** (green) and 870 nm for **12** and **13** (emerald green) typical of copper(II) complexes.

Crystallography

Several crystals of complexes **6**, **7**, **9**, **11** and **12** were mounted on glass fibres for preliminary study. Oscillation and Weissenberg photographs revealed monoclinic unit cells for all five complexes with space group $P2_1/c$ (for **6** and **9**), $P2_1/n$ (for **7** and **12**) or *Cc* (for **11**). X-Ray diffraction data for the refinement of cell parameters and structure determination were collected using a Stoe Stadi-4 four-circle diffractometer with an Oxford Cryosystems open-flow cryostat[16] and ω–θ scans. Data were not collected for **9** ($C_{14}H_{14}Br_2Cl_2CuN_6O_2$, *M* =

620.58, $a = 7.93$, $b = 7.91$, $c = 16.71$ Å, $\beta = 95°$, $U = 1044$ Å^3, $Z = 2$, $D_m = 1.97$, $D_c = 1.974$ g cm^{-3}), owing to its presumed similarity to **6**.

The structures were solved by direct methods (SIR 92[17]) and refined by full-matrix least squares (CRYSTALS[18]) on F^2 using all data. All atoms except hydrogen were allowed anisotropic displacement parameters. For complex **6** all hydrogens were found and refined isotropically. For **7** the cppd hydrogens were found and refined with fixed U_{iso} of 0.03 Å^2. The water hydrogens for **7** and **12** were found but not refined. The cnge hydrogens for **7**, **11** and **12** and the cmppd hydrogens for **11** and **12** were placed and allowed to 'ride' on their parent atoms in calculated positions (X–H 1.00 Å, U_{iso} 0.03 Å^2). Although both tetrafluoroborate anions in **11** were ordered, that in **7** was disordered. The latter was best modelled by two anions, relative occupancies 85 and 15%, disordered about the three-fold axis of symmetry passing through F(21) and B(2). The lower-occupancy fluorines were not refined. Refinement with Chebychev weighting scheme (two parameter for **6**, three parameter for **7**, **11** and **12**) converged to satisfactory conventional R values. Refinement of the two possible enantiomeric forms for **11** gave Flack parameters of 0.38(3) and 0.62(3). Crystal data and details of the determinations are collated in Table 4. All structure diagrams were generated using the CAMERON computing package.[19]

CCDC reference number 186/823.

Acknowledgements

We thank the EPSRC for Post doctoral Research Assistant support and for provision of a four-circle diffractometer and Mr. J. Arnall-Culliford for practical assistance.

References

1 A. D. Burrows, C.-W. Chan, M. M. Chowdhry, J. E. McGrady and D. M. P. Mingos, *Chem. Soc. Rev.*, 1995, **24**, 329; M. J. Zaworotko, *Chem. Soc. Rev.*, 1994, **23**, 283; M. M. Chowdhry, D. M. P. Mingos, A. J. P. White and D. J. Williams, *Chem. Commun.*, 1996, 899; A. D. Burrows, D. M. P. Mingos, A. J. P. White and D. J. Williams, *Chem. Commun.*, 1996, 97; C.-W. Chan, D. M. P. Mingos, A. J. P. White and D. J. Williams, *Chem. Commun.*, 1996, 81; M. Munakata, L. P. Wu, M. Yamamoto, T. Kureda-Sowa and M. Maekawa, *J. Am. Chem. Soc.*, 1996, **118**, 3117; J. Lu, T. Paliwala, S. C. Lim, C. Yu, T. Niu and A. J. Jacobsen, *Inorg. Chem.*, 1997, **36**, 923; S. Sen, S. Mitra, P. Kundu, M. K. Saha, C. Kruger and J. Bruckmann, *Polyhedron*, 1997, **16**, 2475.

2 A. S. Batsanov, P. Hubberstey, C. E. Russell and P. H. Walton, *J. Chem. Soc.*, *Dalton Trans.*, 1997, 2667.

3 A. S. Batsanov, P. Hubberstey and C. E. Russell, *J. Chem. Soc.*, *Dalton Trans.*, 1994, 3189.

4 A. J. Blake, S. J. Hill, P. Hubberstey and W.-S. Li, *J. Chem. Soc.*, *Dalton Trans.*, 1997, 951.

5 P. Hubberstey and J. Stoud, *Polyhedron*, 1997, **16**, 3687.

6 M. J. Begley, P. Hubberstey and J. Stroud, *Polyhedron*, 1997, **16**, 805.

7 A. S. A. G. Tomlinson, B. J. Hathaway, D. E. Billing and P. Nicholls, *J. Chem. Soc. A*, 1969, 65.

8 J. Foley, D. Kennefick, D. Phelan, S. Tyagi and B. J. Hathaway, *J. Chem. Soc.*, *Dalton Trans.*, 1983, 2333.

9 K. Nakamoto, *Infrared and Raman Spectra of Inorganic and Co-ordination Compounds*, 4th edn., Wiley, New York, 1986.

10 M. J. Begley, P. Hubberstey and C. H. M. Moore, *J. Chem. Res.*, 1985, (*S*) 378; (*M*) 4001.

11 A. S. Batsanov, M. J. Begley, P. Hubberstey and J. Stroud, *J. Chem. Soc.*, *Dalton Trans.*, 1996, 1947.

12 M. J. Begley, P. Hubberstey and J. Stroud, *J. Chem. Soc.*, *Dalton Trans.*, 1996, 2323.

13 M. J. Begley, P. Hubberstey and J. Stroud, *Polyhedron*, 1997, **16**, 805.

14 K. Amournjarusiri and B. J. Hathaway, *Acta Crystallogr.*, *Sect. C*, 1991, **47**, 1383; J. Foley, S. Tyagi and B. J. Hathaway, *J. Chem. Soc.*, *Dalton Trans.*, 1984, 1; J. E. Johnson, T. A. Beineke and R. A. Jacobson, *J. Chem. Soc. A*, 1971, 1371.

15 B. J. Hathaway, I. M. Proctor, R. C. Slade and A. A. G. Tomlinson, *J. Chem. Soc. A*, 1969, 2219.

16 J. Cosier and A. M. Glazer, *J. Appl. Crystallogr.*, 1986, **19**, 105.

17 A. Altomare, G. Cascarano, G. Giacovazzo, A. Guagliardi, M. C. Burla, G. Polidori and M. Camalli, *J. Appl. Crystallogr.*, 1994, **27**, 435.

18 D. J. Watkin, C. K. Prout, R. J. Carruthers and P. Betheridge, CRYSTALS, Issue 10, Chemical Crystallography Laboratory, University of Oxford, 1996.

19 D. J. Watkin, C. K. Prout and L. J. Pearce, CAMERON, Chemical Crystallography Laboratory, University of Oxford, 1996.

Received 20*th August* 1997; *Paper* 7/06105F